

Supporting Information for

Lipid Membrane-Assisted Condensation and Assembly of Amphiphilic Janus Particles

Mariah Chambers^{†, #}, Stewart Anthony Mallory^{‡, #}, Heather Malone[†], Yuan Gao[†], Stephen M. Anthony[§], Yi Yi[†], Angelo Cacciuto^{*‡}, and Yan Yu^{*†}

[†] Department of Chemistry, Indiana University, Bloomington, IN 47405, USA

[‡] Department of Chemistry, Columbia University, 3000 Broadway, New York, NY 10027, USA

[§]Department of Bioenergy and Defense Technology, Sandia National Laboratories, Albuquerque, NM 87123, USA

These authors contributed equally.

*Corresponding authors: ac2822@columbia.edu; yy33@indiana.edu

Table of Contents

Experimental Section

Supplementary Figures S1- S4

References

EXPERIMENTAL SECTION

Chemicals and Materials. Monodispersed carboxylate-modified polystyrene microspheres (1.1 μm in diameter, 2% w/v), either fluorescent (red fluorescent, 580/605) or non-fluorescent, were purchased from ThermoFisher Scientific (Waltham, MA). The particles have an average charge density of 2.0×10^6 charges/ μm^2 . Gold pellets for the thermal evaporator were acquired from Kurt J. Lesker (Jefferson Hills, PA). Phospholipid 1,2-dioleoyl-sn-glycero-3-phosphocholine (18:1 (Δ^9 -Cis) PC) (DOPC) was obtained from Avanti Polar Lipid (Alabaster, AL). Phospholipid N-(4,4-difluoro-5,7-dimethyl-4-bora-3a,4a-diaza-s-indacene-3-propionyl)-1,2-dihexadecanoyl-sn-glycero-3-phosphoethanolamine, triethylammonium salt (BODIPY-DHPE) was purchased from ThermoFisher Scientific (Waltham, MA). Sucrose (crystal) was acquired from Avantor Performance Materials (Center Valley, PA).

Fabrication of amphiphilic Janus particles. Carboxylate-modified polystyrene microspheres (1.1 μm) were rinsed with Milli-Q water and re-suspended at a concentration of 2% w/v. This particle concentration was found to be optimal for forming a closely packed monolayer of particles on the glass substrate. Particle monolayers were made using a modified solvent evaporation method.^[1] In brief, 50 μL of particle solution was dropped on a pre-cleaned glass microscope slide. To prevent particle aggregation due to the “coffee stain effect”, continuous convection was applied until the solution dried out. After drying, the particle monolayer was coated with a 5 nm thick layer of chromium, and a 30 nm thick layer of gold using an Edwards thermal evaporation system (Nanoscale Characterization Facility, Indiana University). Immediately after being coated with metal, the particle monolayers were immersed in ethanol containing 2 mM 1-octadecanethiol for 2 hours to make the gold coating hydrophobic. After thiol functionalization, the particle monolayer was rinsed thoroughly with ethanol containing 2% HCl to remove non-specifically adsorbed thiols. Janus particles were removed from microscope slides by sonication prior to use.

Preparation of giant unilamellar vesicles (GUVs). GUVs were prepared using the gentle hydration method.^[2] DOPC and BODIPY-DHPE were mixed in chloroform at a molar ratio of 1000:1 to reach a final concentration of 1 mg/mL and 1 $\mu\text{g/mL}$, respectively. The mixture (500 μL) was dried into a uniform lipid film in a round bottom flask via a rotary evaporator. Janus particles at an estimated concentration of 2.43×10^8 particles/mL were suspended in sucrose solution (100 mM, 5 mL) and added to the dried lipid film without disturbing the lipid layer. In experiments where the rotation of single particles was measured, fluorescent and non-fluorescent carboxylate-modified polystyrene particles were mixed at a molar ratio of $\approx 1:100$. The lipid sample was incubated at 40°C overnight for hydration.

Fluorescence imaging. GUVs were imaged at room temperature using a Nikon Eclipse fluorescence microscope that is equipped with an Andor iXon3 EMCCD camera and a Nikon Plan Apo 100 \times /1.49 N.A oil immersion objective.

Analysis of rotation of single Janus particles. The azimuthal (in-plane) and polar (out-of-plane) angle of single Janus particles were measured from fluorescence images using a previously reported algorithm with slight modification.^[3] Briefly, the first step after noise reduction was to identify the centroid of each particle. An intensity-based contour plot was made for the fluorescence image of each particle. Each contour plot consisted of nested semicircles except when the particle was in “full moon” orientation with the fluorescent hemisphere completely facing the microscope detector. Using a curve-fitting algorithm, a circle was fitted to each of the outermost five contours for each particle. The median of the x- and y-coordinates of the five identified centroids was computed as an estimate of the location of the particle centroid. The second step was to determine the azimuthal angle ϕ . An ellipse was fitted, using intensity weighting, to the fluorescence image of each particle. The orientation of the minor axis of each ellipse was obtained as an estimate of ϕ . Next, the polar angle θ was determined from the intensity (I) of the

fluorescent hemisphere using the equation: $I = \frac{I_{max}}{2} \cdot (1 + \cos\theta)$. In this equation, I_{max} is the fluorescence intensity for $\theta = 0$, which is the "full moon" orientation. Because in the experiments each rotating particle experiences all possible orientations during the imaging time window, I_{max} was obtained from the maximum intensity exhibited by a given particle. The next step was to compute the translational trajectory of single particles as projected on the image plane. This was done by connecting the centroids of particles from one frame to the next, under the condition that the translational displacement of each particle between frames was smaller than its radius. The combination of each particle's azimuthal angle ϕ and polar angle θ was treated as a point in a two-dimensional Cartesian space. The frame-to-frame displacement of this point between any two images was a measure of rotational displacement, and used to calculate the rotational speed. The tracking inaccuracy of the rotational speed was estimated to be 0.1 rad/s.

Simulations. The amphiphilic nature of the Janus particles was modeled by placing $K = 72$ distinct spheres of diameter σ at the vertices of an icosadeltahedral configuration over the spherical surface of each Janus particle. The bare radius of a Janus particle was set to 1σ . However, the effective radius of the simulated Janus particle becomes $R_j = 1.5\sigma$, when including the radius of the spheres placed on the configuration surface. A suitably large number of spheres was chosen to reproduce accurately the shape of the particle and to make its surface sufficiently smooth. We denoted the spheres that make up the hydrophobic and hydrophilic hemisphere of each model Janus particle as type A and type B, respectively. A short-ranged attraction between the hydrophobic hemispheres was realized by having particles of type A interact via a shifted Lennard-Jones potential:

$$V_{AA}(r) = 4\varepsilon_{AA} \left[\left(\frac{\sigma}{r} \right)^{12} - \left(\frac{\sigma}{r} \right)^6 + \frac{1}{4} \right]$$

In this equation, the range of interaction extends out to $r_c = 2.5\sigma$. Here r is the distance between any two spheres of type A on different colloidal particles. The strength of the overall attraction was modulated by the pairwise interaction energy ε_{AA} . The remaining pair interactions, namely V_{AB} and V_{BB} , are described using the purely short-range repulsive interaction provided by the Weeks Chandler Andersen (WCA) potential, which has the same form as the shifted Lennard-Jones potential but with range of interaction truncated at $r_c = 2^{1/6}\sigma$. The spheres within the same Janus particle are held fixed to form the surface of the particle, and do not interact with one another. The total pair energy as a function of distance, d , for two Janus particles with the hydrophobic hemispheres facing each other at different values of ε_{AA} is given in **Figure S3a**. In our simulation, we considered values of the interaction energy ε_{AA} such that the overall attraction between Janus particles is no larger than a few $k_B T$. This is consistent with the experimental observation that the Janus particles observed in this study do not spontaneously aggregate into large linear clusters in the bulk.

In our simulations, the membrane was represented as a rigid surface built out of a large number of spheres of diameter $\sigma=1$ arranged into an hexagonal lattice (with the distance between the vertices of the lattice being σ). We used two different approaches to modeling the interaction between Janus particles and the membrane. The simplest approach assumed that the Janus particles were isotropically attracted to the membrane surface. In this case, the interaction between the center of the Janus particle and the spheres composing the membrane was described by a Yukawa-like potential of the form:

$$V_w(r) = -g^2 \frac{e^{-\kappa r}}{r}$$

In this equation g and κ control the strength and range of the interaction, respectively, and r is the center-to-center distance between the Janus particle and a membrane sphere. The pair energy for a single Janus particle as a function of distance above the surface is given in **Figure S3b** for several values of κ .

The second approach to modeling the Janus particle-membrane interaction assumed the attractive interaction between the Janus particle and the membrane was due specifically to the hydrophilic hemisphere. In this case the interaction acted only on the spheres in the membrane and those on the hydrophilic hemisphere of the Janus particles via the potential:

$$V_w(r) = -g_i^2 \frac{e^{-\kappa r}}{r}$$

The value of g_i for the type B spheres composing the hydrophilic region of the Janus particle was selected so that the overall strength and shape of the potential is comparable to that adopted in the first (isotropic) approach. We set $g_i = 0$ for the type A spheres forming the hydrophobic side of the particles. The total pair energy, as calculated with these assumptions, for a single Janus particle with its hydrophilic hemisphere facing the surface is given in **Figure S3c** for several values of κ .

The equations of motion for both the rotation and translation of a single Janus particle are given by the Langevin equations:

$$m\ddot{\mathbf{r}} = -\gamma\dot{\mathbf{r}} - \partial_r V + \sqrt{2\gamma^2 D} \xi(t)$$

$$\dot{\mathbf{n}} = -\frac{D_r}{k_B T} \nabla_n V(r) + \sqrt{2D_r} \xi_r(t) \times \mathbf{n}$$

In these equations, γ is the translational friction and V is the pair potential acting on the particles, and \mathbf{n} is a predefined orientation vector, which passes through the origin of each Janus particle and connects its poles. The translational and rotational diffusion constants are given by D and D_r , respectively. The solvent-induced Gaussian white noise terms are characterized by $\langle \xi_i(t) \rangle = 0$ and $\langle \xi_i(t) \cdot \xi_j(t') \rangle = \delta_{ij} \delta(t - t')$ for the translational motion, and $\langle \xi_{ri}(t) \rangle = 0$ and $\langle \xi_{ri}(t) \cdot \xi_{rj}(t') \rangle = \delta_{ij} \delta(t - t')$ for the rotational motion. The translational diffusion constant D is related to the temperature T via the Stokes-Einstein relation $D = k_B T / \gamma$. In the low Reynolds number regime, the rotational and translational diffusion coefficients for a sphere satisfy the relation $D_r = 3D / \sigma_j^2$. The Janus particle and its surface spheres are treated as a single rigid body.

All simulations were carried out using the numerical package LAMMPS in a cubic box of linear dimension $L = 20$ with periodic boundary conditions in the directions parallel to the membrane surface with $N = 100$ Janus particles. Each Janus particle has an effective diameter $\sigma_j = 3$, mass $m = 1$, and undergoes Langevin dynamics at constant temperature $T = 1$. The remaining parameters are set such that $g = 5$, $\epsilon_{AB} = \epsilon_{AB} = 1$, and $\sigma = 1$. Each simulation was run for a minimum of 10^6 time steps with time step size $dt = 0.001$. All results pertaining to simulations are given in standard reduced Lennard-Jones units.

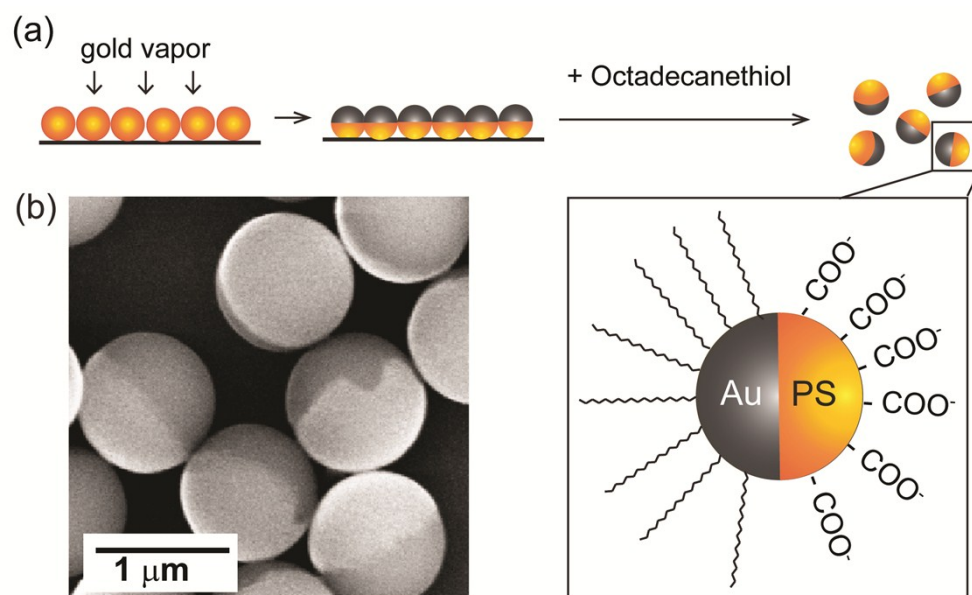


Figure S1. (a) Schematic illustration of the fabrication of amphiphilic Janus particles. A monolayer of 1- μm polystyrene (PS) particles displaying carboxylate groups was coated with a 5 nm thick layer of chromium, and a 30 nm thick layer of gold via directional deposition. The gold side was conjugated with 1-octadecanethiol to become hydrophobic. (b) Scanning electron microscopy (SEM) image of the amphiphilic Janus particles.

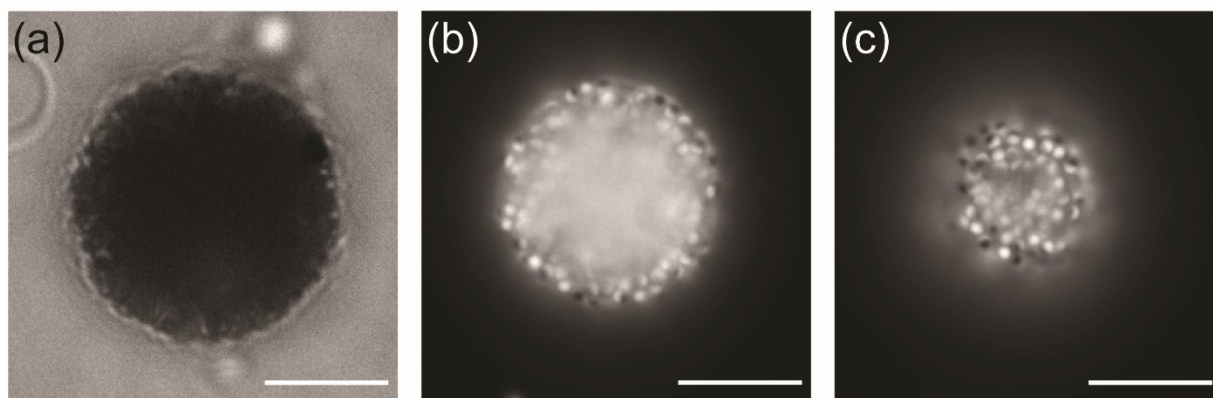


Figure S2. Condensation of Janus particles on a GUV membrane when particle concentration in the solution was lowered by tenfold to 2.43×10^7 particles/mL. (a) Bright-field image showing Janus particles inside a GUV. The particles appear dark because their metal coatings block transmitted light. (b-c) Fluorescence images showing the Janus particles inside near the equator of the GUV (b) and at the bottom of the GUV (c). Scale bars: 10 μm .

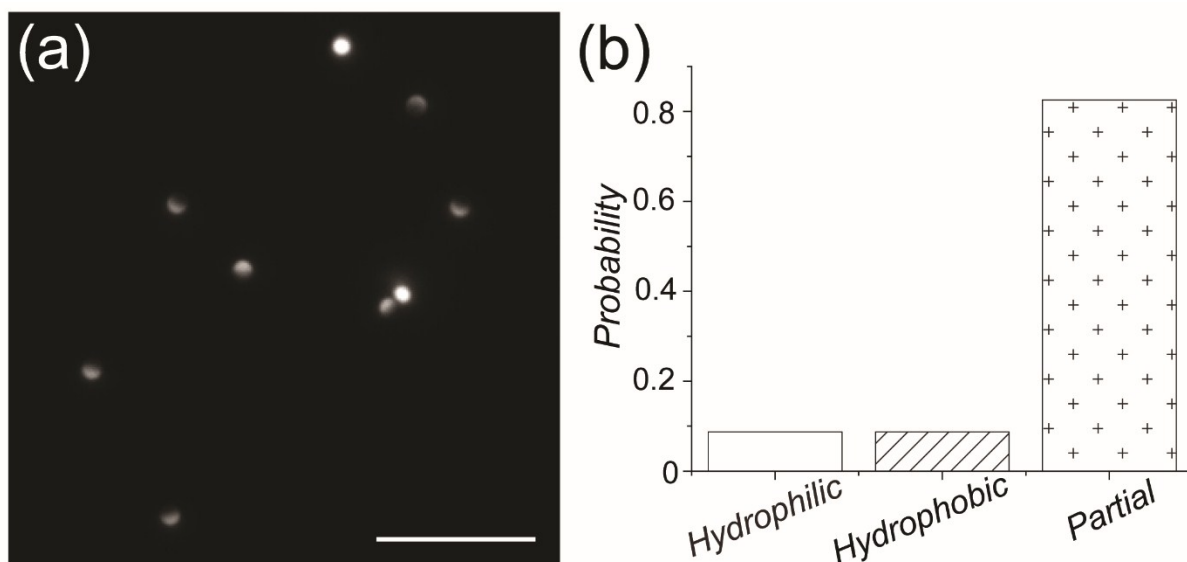


Figure S3. Orientation of Janus particles on surface-supported planar lipid bilayers. (a) A fluorescence image showing the dispersed Janus particles on a lipid bilayer. Scale bar: 10 μm . (b) Histogram from 126 particles showing the probabilities of particle orientation with respect to the GUV membrane. Orientation was defined in three categories: particles with the fluorescent hydrophilic hemisphere (hydrophilic) facing completely towards the GUV membrane, ones with the gold-coated hydrophobic side (hydrophobic) completely facing the membrane, or with the interface facing the membrane (partial).

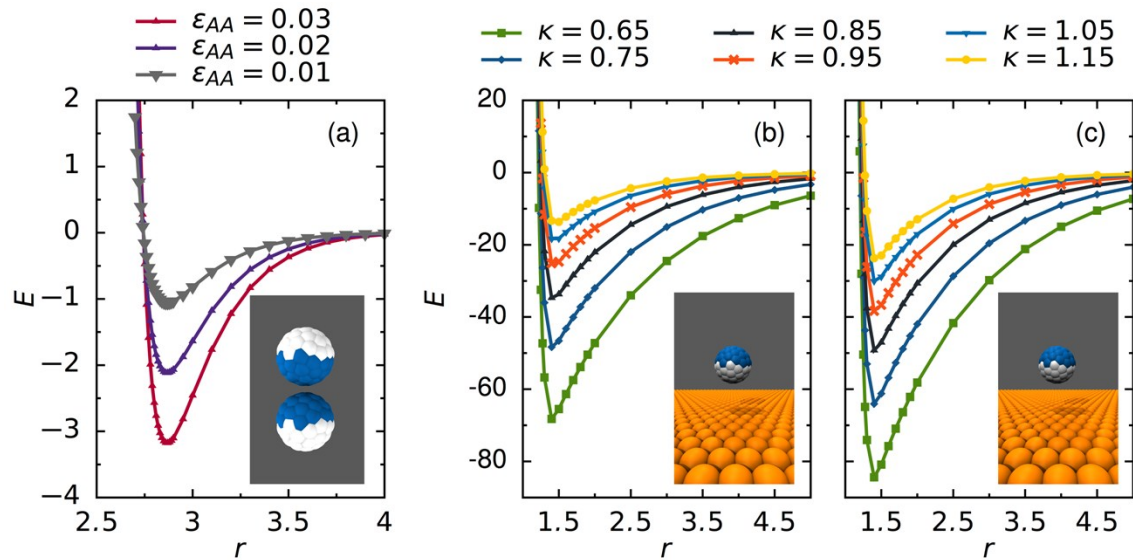


Figure S4. (a) Pair energy for two simulated Janus particles with attractive hydrophobic patches (blue) aligned plotted as a function of distance. Pair energy as a function of distance above the membrane for different values of κ where simulated Janus particles are isotropically attracted to the membrane (b) and where only the hydrophilic hemispheres (white) are attracted to the membrane (c).

References

- [1] A. S. Dimitrov, K. Nagayama, *Langmuir* **1996**, *12*, 1303-1311.
- [2] K. Akashi, H. Miyata, H. Itoh, K. Kinoshita, Jr., *Biophys. J.* **1998**, *74*, 2973-2982.
- [3] aS. M. Anthony, L. Hong, M. Kim, S. Granick, *Langmuir* **2006**, *22*, 9812-9815; bS. M. Anthony, M. Kim, S. Granick, *Langmuir* **2008**, *24*, 6557-6561.